Quantifying exciton hopping in disordered media with quenching sites: Application to arrays of quantum dots

Jun Miyazaki*

Advanced Ultrafast Laser Research Center, University of Electro-Communications, Chofugaoka 1-5-1, Chofu, Tokyo 182-8585, Japan

(Received 20 May 2013; revised manuscript received 22 July 2013; published 4 October 2013)

We present an analytical method for quantifying exciton hopping in an energetically disordered system with quenching sites. The method is subsequently used to provide a quantitative understanding of exciton hopping in a quantum dot (QD) array. Several statistical quantities that characterize the dynamics (survival probability, average number of distinct sites visited, average hopping distance, and average hopping rate in the initial stage) are obtained experimentally by measuring time-resolved fluorescence intensities at various temperatures. The time evolution of these quantities suggests in a quantitative way that at low temperature an exciton tends to be trapped at a local low-energy site, while at room temperature, exciton hopping occurs repeatedly, leading to a large hopping distance. This method will serve to facilitate highly efficient optoelectronic devices using QDs such as photovoltaic cells and light-emitting diodes, since exciton hopping is considered to strongly influence their operational parameters. The presence of a dark QD (quenching site) that exhibits fast decay is also quantified.

DOI: 10.1103/PhysRevB.88.155302 PACS number(s): 78.67.Hc, 78.55.Qr, 66.30.Pa, 71.35.−y

I. INTRODUCTION

The optical properties of semiconductor quantum dot (QD) aggregates can be harnessed for optoelectronic devices such as photovoltaic cells,[1–3] light-emitting diodes,[4–7] and photodetectors.[8–10] The excitation energy transfer in these types of materials usually occurs between adjacent QDs owing to electronic coupling, and this process is considered to strongly influence their operational parameters. Several experimental studies have shown that in spatially separated QDs energy is transferred from small to large QDs, corresponding to a high-to-low excitonic energy state that is reflected clearly in the fluorescence intensity in both the temporal and spectral domains.[11–18] In a mixture of two different-sized QD ensembles, for example, the ratio of the fluorescence intensity of the donor to that of the acceptor decreases over time owing to the energy transfer.

In a monodispersed QD ensemble, a dynamic fluorescence redshift appears because spectral broadening arises from the size distribution of the individual QDs in the ensemble (inhomogeneous broadening), and energy transfer occurs repeatedly to a site of low energy (exciton hopping).[11,13,17,18] We recently studied the dynamics of exciton hopping in an array of inhomogeneously broadened CdSe/ZnS QDs by measuring the time-resolved and spectrally resolved fluorescence intensities.[19,20] We found that excitons tend to be trapped in a local low-energy site at low temperature, while the hopping probability increases as the temperature increases.[19] Furthermore, the exciton dynamics was found to depend on the initial exciton energy.[20] The findings also suggested that there are dark QDs associated with the defect and/or off state of blinking QDs in the ensemble, and the energy transfer to such a site is followed mainly by quenching, which leads to a decrease in the fluorescence intensity. These results may give some general insight into realizing nanocrystal optoelectronic devices; however, they provided only a qualitative understanding and further quantitative evaluation is required.

Similar processes have been reported in inhomogeneously broadened conjugated polymers.[21–25] Exciton hopping and the resulting quenching and/or dissociation in conjugated polymers is of major concern for realizing highly efficient organic electronic components such as photovoltaic cells and light-emitting diodes. In a photovoltaic cell, the photoexcited exciton is transported to an interface at which charge separation takes place; a long transport length is usually desired to improve the dissociation efficiency. For organic light-emitting diodes, however, exciton quenching by impurities or other quenching centers reduces the photoconversion efficiency.[21] In a light-harvesting system, this process is utilized as a photoprotection mechanism in which molecules such as carotenoids dissipate excess energy as heat to avoid the generation of toxic photo-oxidative intermediates.[26–28]

In systems with energetic disorder, exciton hopping accompanies energy relaxation (exciton transfer occurs preferentially from a high- to low-energy state), and thus the hopping probability decreases as it reaches a low-energy site. It is therefore not possible to describe exciton hopping using a constant diffusion coefficient, which makes the analysis more complicated. In the case of charged carriers, emphasis has been given to the relationship between the diffusion coefficient and the mobility in a disordered system in the presence of an external field,[29–33] and it has been claimed that the conventional Einstein relation is violated in the nonequilibrium state. To date, there have been several numerical and analytical studies dealing with hopping dynamics in disordered media with quenching sites that used the Monte Carlo method or solved a master equation,[34–38] but little use has been made of experimental observables.

Here, we develop an analytical method to experimentally evaluate the dynamics of exciton hopping in a system with energy disorder and quenching sites. The method provides a direct quantitative understanding of exciton hopping in a QD array. Several statistical quantities such as the survival probability, the average number of distinct sites visited, the average hopping distance, and the average hopping rate are obtained by measuring the time-resolved fluorescence intensity at various temperatures, which enables us to discuss temperature-dependent exciton hopping in a quantitative way.

II. THEORETICAL CONSIDERATIONS

We first consider a random walk on an array with energy disorder in the presence of quenching sites as a model of exciton hopping in a QD array [see schematic in Fig. 1(a)]. The energy disorder is considered to originate from the size distribution in the QD ensemble, and we assume that the quenching sites are a result of defects or excess charges randomly distributed on the surface of the QD array with a probability of γ. When an exciton reaches a quenching site, it stops and is then annihilated. The quenching site plays the same role as the deep trap in a semiconductor acting as a recombination center for charge carriers.[34,39–47]

The time dependence of the survival probability $\rho(t)$, which is the average probability of an exciton not reaching the quenching site by time t, is an important statistical quantity for characterizing this random walk. The random walk is also characterized by the number of distinct sites $S(t)$ visited after time t, which is related to $\rho(t)$ by

$$\rho(t) = \langle (1-\gamma)^{S(t)} \rangle, \tag{1}$$

where $\langle \cdots \rangle$ denotes the average over the subspace of excitons that have survived at t for all possible quenching site and disorder configurations.

When there is no energy disorder and the exciton hopping rate is constant for all pairs of neighboring sites, Eq. (1) is well approximated over a short time range and for small γ by expanding and truncating the equation up to the first-order cumulant;[39,42]

$$\rho(t) = (1-\gamma)^{\langle S(t) \rangle}. \tag{2}$$

In dimensions higher than two, $\langle S(t) \rangle$ is proportional to t, and thus $\rho(t)$ exhibits an exponential dependence on t. In two dimensions (2D), a logarithmic correction appears in the denominator, $\langle S(t) \rangle \propto t/\ln(t)$, while in one dimension (1D), $\langle S(t) \rangle \propto \sqrt{t}$.

In the presence of energetic disorder, however, the exciton is trapped at a local low-energy site, and thus the probability distribution of $S(t)$ is likely to be broad with respect to t. Equation (2) is therefore valid only for small values of t or, equivalently, a small $S(t)$. Several analytical approaches have been developed to deal with such cases,[34–38] and quenching of excitons in conjugated polymers have been explained in this context.[22,23]

In the present study, to provide a quantitative understanding of the exciton hopping dynamics in a disordered system, we instead consider the quantity $\langle S(t) \rangle^*$; i.e., $S(t)$ averaged over all excitons (quenched and unquenched). Here we assume that $S(t)$ is constant after an exciton reaches a quenching site; if an exciton has visited $n-1$ sites before reaching a quenching site at t', then $S(t) = n$ for $t > t'$. In this case, $\rho(t)$ is related to $\langle S(t) \rangle^*$ through $d\rho(t)/dt = -\gamma d\langle S(t) \rangle^*/dt$, and consequently we obtain

$$\langle S(t) \rangle^* = [1-\rho(t)]/\gamma. \tag{3}$$

This relation holds for any value of t provided that the quenching sites are randomly distributed. In the experiment, since $\rho(t)$ can be extracted from time-resolved fluorescence intensities, as detailed in the following section, $\langle S(t) \rangle^*$ is obtained experimentally by using Eq. (3).

Monte Carlo simulations of the random walk on an array with energetic disorder and quenching sites were conducted to examine the time evolution of both $\rho(t)$ and $\langle S(t) \rangle^*$. The exciton hopping mechanism is attributed to interdot dipole-dipole coupling, known as the Förster mechanism.[15] For a energetically disordered medium, the hopping rate of an exciton at site i with an energy ϵ_i jumping to a neighboring site j is frequently calculated using[22,34,48,49]

$$w_{ij} = \chi P(\epsilon_i, \epsilon_j), \tag{4}$$

where

$$\chi = (1/\tau_R)(R_F/d)^6,$$
$$P(\epsilon_i, \epsilon_j) = \begin{cases} 1, & \epsilon_i > \epsilon_j \\ \exp[-(\epsilon_j - \epsilon_i)/kT], & \epsilon_i < \epsilon_j, \end{cases} \tag{5}$$

where ϵ_j is the energy level of site j, τ_R is the radiative lifetime, R_F is the Förster radius, k is the Boltzmann constant, and T is the temperature. We assume that the distance between each neighboring site d is constant, and only nearest-neighbor coupling is taken into account. Furthermore, for simplicity, we do not consider the orientational factor between dipoles and assume the same R_F for adjacent QD pairs. The inhomogeneous broadening of the energy level ϵ_n is given by a Gaussian with a width of $\sigma = 33$ meV, which corresponds to the experimental result.[19] The energy levels of all sites including the initial site are randomly assigned according to a Gaussian probability. This situation corresponds to the case in which all the QDs are equally excited irrespective of their size. The initial site is assumed not to be a quenching site since we consider the hopping dynamics of an exciton that is photoexcited in a bright (nonquenching) site. For convenience, we set $\chi = 1/N$ in the numerical calculation, with N being the number of neighboring sites, so that for each Monte Carlo step, the exciton either jumps from site i to a neighboring site j with a probability of w_{ij}, or the exciton stays at site i with a residual probability of $1 - \sum_j^N w_{ij}$. The Monte Carlo step is repeated until an exciton reaches a quenching site.

Figure 1 shows $\rho(t)$ as a function of the number of Monte Carlo steps at different temperatures in a 2D array with hexagonal order. To examine how $\rho(t)$ depends on the number of dark QDs, γ is set to 0.1 and 0.7 in Figs. 1(a) and 1(b), respectively. We can see clearly that $\rho(t)$ decreases with increasing temperature. At $T = 0$ (K), after several steps, the exciton is trapped at the local low-energy site, so that $\rho(t)$ remains constant over time. In contrast, for a nonzero temperature, an exciton will eventually reach a dark site, and $\rho(t)$ then approaches zero in the long-time limit. In the high-temperature limit (HTL), the hopping probability is constant for all pairs of neighboring sites, which is equivalent to the case in which there is no energy disorder. Figure 1(c) shows that, after several steps, $\rho(t)$ decreases significantly for a large γ, since an exciton easily reaches a dark site.

Figure 2 shows that there is good agreement between $\langle S(t) \rangle^*$ and the right-hand side of Eq. (3). Although the energy level of the initial site is randomly assigned, Eq. (3) holds irrespective of the initial energy level. The probability distribution of $S(t)$ approaches an exponential with an average of $1/\gamma$ in the long-time limit except for the case in which $T = 0$ (K). Note that, for a large γ, $S(t)$ nearly saturates at around $1/\gamma$ after several

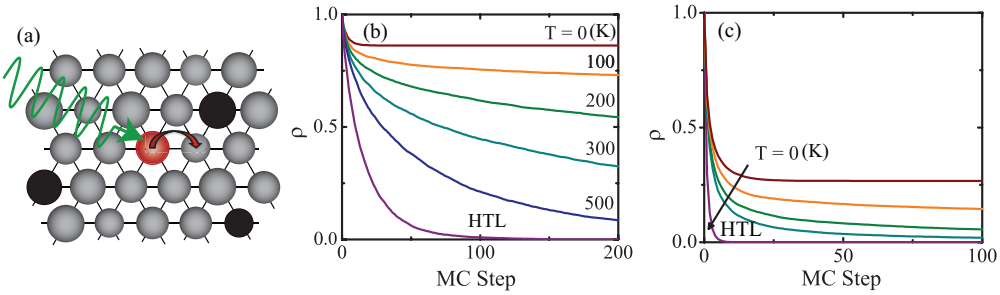

FIG. 1. (Color online) (a) Exciton hopping model on an hexagonal array with energy disorder in the presence of quenching sites. Filled circles denote the quenching sites randomly distributed in the array with a probability of γ. (b), (c) Survival probability $\rho(t)$ at various temperatures for a 2D array with hexagonal order. The proportion of quenching sites γ was set to 0.1 and 0.7 in (b) and (c), respectively. The survival probability is shown for temperatures of 0, 100, 200, and 300 K, as well as the high-temperature limit (HTL), i.e., infinite temperature.

steps. This indicates that, for a large γ, there is little hopping after several steps as an exciton reaches a dark site.

The time dependence of the hopping distance $L(t)$ of an exciton relative to the initial position also gives some insight into the dynamics. To obtain the average hopping distance $\langle L(t)\rangle^*$ from experimental observables, we consider the relationship between L and S. Suppose that an exciton has just visited the sth distinct site. At this moment, the hopping distance $\langle L\rangle_s$ averaged over all possible paths while holding s constant is calculated in the 1D system as (see Appendix A)

$$\langle L\rangle_s = d[(2/3)s + 1/3], \tag{6}$$

where we have assumed that every path with the same number of hops has the same probability of occurring. This assumption is valid even for a disordered system when averaging over disordered configurations. The relationship between $\langle L(t)\rangle^*$ and $\langle S(t)\rangle^*$ is then obtained by replacing s in Eq. (6) with $S(t)$ and taking the average. However, since there is a probability that the exciton returns to a previously visited site, $\langle L(t)\rangle^*$ is usually smaller than $\langle\langle L\rangle_{s(t)}\rangle^*$. Consequently, we obtain the relation

$$\langle L(t)\rangle^* \lesssim d[(2/3)\langle S(t)\rangle^* + 1/3]. \tag{7}$$

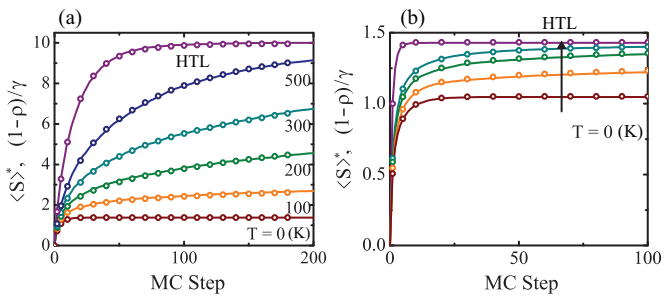

FIG. 2. (Color online) Average number of distinct sites visited, $\langle S(t)\rangle^*$, for various temperatures in the case of a 2D array with hexagonal order. The proportion of quenching sites γ was set to 0.1 and 0.7 in (a) and (b), respectively. Results shown in panel (b) are for temperatures of 0, 100, 200, and 300 K, as well as the HTL. The solid lines in panels (a) and (b) are obtained by substituting the values of $\rho(t)$ in Figs. 1(b) and 1(c) into to the right-hand side of Eq. (3), respectively, while the open circles are the simulated values of $\langle S(t)\rangle^*$.

For dimensions higher than or equal to two, numerical simulations showed that $\langle L\rangle_s$ is well approximated by

$$\langle L\rangle_s \sim ds^\alpha, \tag{8}$$

as shown in Fig. 3(a). The exponent α is equal to 0.57 and 0.56 for 2D square and hexagonal lattices, respectively, and for the three-dimensional (3D) primitive cubic lattice, $\alpha = 0.55$. By using the approximation $\langle s^\alpha\rangle^* \sim \langle s\rangle^{*\alpha}$, we obtain

$$\langle L(t)\rangle^* \lesssim d\langle S(t)\rangle^{*\alpha}. \tag{9}$$

Figures 3(b) and 3(c) present the results of the Monte Carlo simulation, which show the relationship between the average hopping distance normalized by the interdot distance, i.e., $\langle L(t)\rangle^*/d$, and $\langle S(t)\rangle^{*\alpha}$ for various temperatures in the case of a 2D array with hexagonal order. Although $\langle S(t)\rangle^{*\alpha}$ overestimates $\langle L(t)\rangle^*/d$ by about 10%, it gives a fairly good approximation of $\langle L(t)\rangle^*/d$. For a large γ, $\langle L(t)\rangle^*/d$ nearly saturates after several steps because an exciton is quenched at a dark site in the vicinity of the initial site.

In the experiment, since $\langle S(t)\rangle^*$ is given by Eq. (3), approximate values of $\langle L(t)\rangle^*$ are obtained from Eqs. (7) or (9) depending on the dimensions and lattice configuration. However, α in Eq. (9) does not appear to be sensitive to the lattice configuration in dimensions higher than or equal to two.

It is important to determine γ so that $\langle S(t)\rangle^*$ can be calculated from $\rho(t)$ via Eq. (3). When there is a large proportion of quenching sites in the ensemble, γ can be estimated directly by measuring fast relaxation in time-resolved spectroscopy, as described in the following section. However, to quantify small γ, we consider the asymptotic (long-time limit) value of $\langle S(t)\rangle$ at low temperatures ($kT \ll \sigma$) for which exciton hopping is mainly from a high- to low-energy site before trapping occurs. In this case, $\langle S(t)\rangle$ converges asymptotically to a finite value $S_{\rm inf}$ in the long-time limit. For a 1D system at zero temperature, the analytical solution is

$$S_{\rm inf} = \sum_{n=1}^{\infty} \frac{[\mathrm{erf}(\epsilon)+1]^n[2n+1-\mathrm{erf}(\epsilon)][3-\mathrm{erf}(\epsilon)]n}{2^{n+2}(n+1)!}, \tag{10}$$

where $\epsilon = \epsilon_0/\sigma$, and ϵ_0 is the energy level of the initial site. The derivation of Eq. (10) is described in Appendix B. When the initial energy level is sufficiently large, i.e., $\epsilon \gg 1$, $S_{\rm inf}$ approaches $e-1$, but for $\epsilon \ll 1$, an exciton is trapped at the

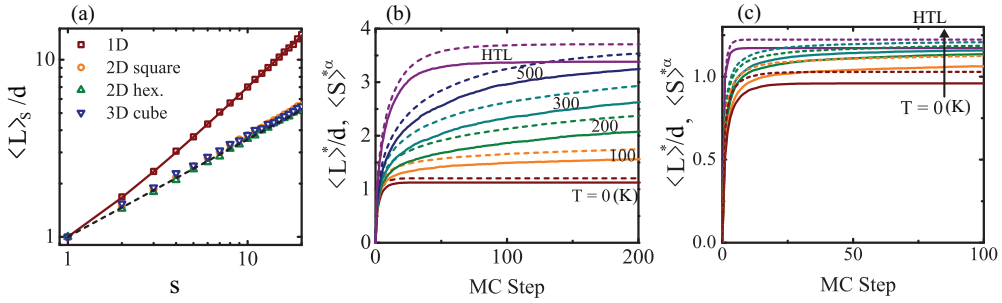

FIG. 3. (Color online) (a) Normalized hopping distance $\langle L\rangle_s/d$ averaged over all possible paths for a constant s for several dimensions and lattice configurations; 1D: brown squares, 2D square (hexagonal) lattice: orange circles (green triangles), and 3D cubic lattice: blue inverted triangles. The solid line denotes the theoretical curve for the 1D system $(2/3)s + 1/3$, and $\langle L\rangle_s/d$ for the 2D and 3D lattices is well fit by s^α; e.g., for the 2D array with hexagonal order, $\alpha = 0.56$ (dashed line). (b), (c) Time courses of $\langle L(t)\rangle^*/d$ (solid lines) and $\langle S(t)\rangle^{*\alpha}$ (dashed lines) for various temperatures for a 2D array with hexagonal order, with γ set to 0.1 and 0.7 in panels (b) and (c), respectively.

initial site so that $S_{\rm inf}$ is zero. For dimensions higher than or equal to two, we obtained $S_{\rm inf}$ from numerical calculations. Figure 4 shows $S_{\rm inf}$ as a function of ϵ for several dimensions and lattice configurations. In the 2D system, $S_{\rm inf}$ approaches 2.41 and 2.75 for large ϵ in the square and hexagonal lattices, respectively, while $S_{\rm inf}$ approaches 2.82 in the 3D primitive cubic lattice system. By assuming that Eq. (2) holds for small values of $\langle S(t)\rangle$ and γ, we note that

$$\gamma \sim 1 - \rho_{\rm inf}^{1/S_{\rm inf}}, \tag{11}$$

where $\rho_{\rm inf}$ is the asymptotic value of $\rho(t)$ in the limit $t \to \infty$. Therefore, γ can be determined by substituting the experimentally measured $\rho_{\rm inf}$ value and the analytically or numerical calculated $S_{\rm inf}$ value into Eq. (11).

In some experiments, all the QDs are equally excited irrespective of the energy level,[19] and in this case, $S_{\rm inf}$ should be averaged over ϵ_0 to give $\tilde{S}_{\rm inf}$. The numerical calculations give $\tilde{S}_{\rm inf}$ as 1.48 and 1.81 for the 2D square and hexagonal lattices, respectively, and 1.91 for the 3D primitive cubic lattice.

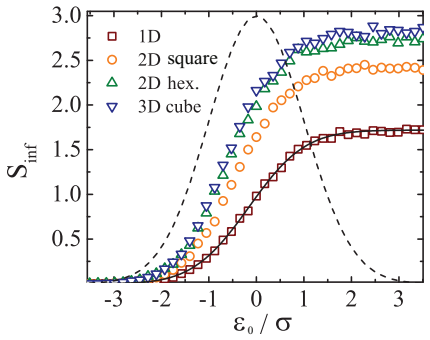

FIG. 4. (Color online) Asymptotic values of the average number of distinct sites visited, $S_{\rm inf}$, in the long-time limit at zero temperature as a function of the energy level of the initial site ϵ_0. $S_{\rm inf}$ is obtained from numerical calculations for several dimensions and lattice configurations; 1D: brown squares, 2D square (hexagonal) lattice: orange circles (green triangles), and 3D cubic lattice: blue inverted triangles. The solid line is the theoretical curve for the 1D system given by Eq. (10). The dashed line denotes the inhomogeneous distribution of the energy levels, and the horizontal axis is normalized by the width σ.

The procedure for quantifying exciton hopping from experimental observables is summarized as follows:

(1) The survival probability $\rho(t)$ can be extracted from time-resolved fluorescence intensities, as detailed in the following section.

(2) When there is a large proportion of quenching sites in the ensemble, γ can be estimated directly by measuring fast relaxation in time-resolved spectroscopy. In the case of small γ, an estimation is obtained via Eq. (11) using $\rho_{\rm inf}$ and $S_{\rm inf}$, where $\rho_{\rm inf}$ is obtained experimentally from the asymptotic values of $\rho(t)$ at low temperature. In contrast, $S_{\rm inf}$ is given analytically by Eq. (10) for a 1D system and obtained from numerical calculations for dimensions higher than or equal to two. Since $S_{\rm inf}$ depends on the energy level of the initial site as shown in Fig. 4, it is convenient to measure $\rho(t)$ for various initial energy levels to determine $\rho_{\rm inf}$. In the experiment, the initial energy level can be tuned by changing the excitation photon energy at the absorption edge.[19]

(3) The average number of distinct sites visited, $\langle S(t)\rangle^*$, is then calculated by substituting $\rho(t)$ and γ into Eq. (3). The approximate value of the hopping distance is given via Eqs. (7) or (9) using $\langle S(t)\rangle^*$.

What is new in the present analysis is that we consider $\langle S(t)\rangle^*$ instead of $\langle S(t)\rangle$ to deal with the disordered system and subsequently obtain a relation between $\langle S(t)\rangle^*$ and the average hopping distance. We also present a method to quantify small γ using $\rho_{\rm inf}$ and $S_{\rm inf}$. This method is valid when the quenching sites are randomly distributed and an exciton is inevitably annihilated after it reaches the quenching site. However, this method is independent of the detailed characteristics of the hopping mechanism, even though we have employed the model described by Eqs. (4) and (5) in the Monte Carlo simulation.

In the present study, we considered the hopping dynamics of an exciton that is photoexcited in a bright site and therefore the initial site is assumed not to be a quenching site as described above. However, the present method is valid even when all excitons (photoexcited in both the bright and quenching site) are considered. In this case, $\rho(t)$ and $\langle S(t)\rangle^*$ should be replaced with $(1-\gamma)\rho(t)$ and $(1-\gamma)\langle S(t)\rangle^*$, respectively.

In the following sections, we apply this analytical method to exciton hopping in QD arrays.

III. METHODS AND MATERIALS

An optical parametric amplifier pumped by a 1 kHz regenerative Ti:sapphire laser was employed as the light source. The tunable range of the excitation photon energy was 1.9 to 3.5 eV. A grating pair and slit were employed to reduce the bandwidth of the pulse to a full width at half maximum (FWHM) of less than 2 nm. The power density of the excitation pulse was sufficiently weak (20 nJ/cm^2) to avoid multi-exciton generation in a single QD.

A streak camera (Hamamatsu C4780) and monochromator (Chromex 250is) were employed to obtain the time- and spectrally resolved fluorescence intensities with a wavelength resolution of 0.9 nm. The measuring time ranges were 50 ns, and typical time resolutions were 0.6 ns. The absorption spectra of the QD samples were measured using a spectrophotometer equipped with an integrating sphere (JASCO V-670). The sample temperature was controlled either by a transparent glass dewar or a liquid-nitrogen cryostat system (Janis Research VNF-100) over a temperature range of 80–294 K (room temperature).

The CdSe/ZnS core/shell nanocrystals capped with octadecylamine were purchased from NN Labs, Inc. and have a fluorescence peak at 2.14 eV (580 nm) and a fluorescence quantum yield of approximately 50%. The QD arrays were prepared by dropping the fresh sample in toluene onto a quartz plate under an argon atmosphere. The sample was then dried under vacuum for several hours to evaporate the solvent. From transmission electron microscopy (TEM) measurements, we confirmed that the QD ensemble forms a 2D close-packed network with hexagonal order. We also prepared a solid QD dispersion consisting of the QDs embedded in octadecylamine as a control sample.

Observation of the edge excitation redshift (EERS) by varying the excitation photon energy at the absorption edge[19,20] clarified the width of the inhomogeneous distribution in the QD ensemble to be 33 meV.

In order to examine the dependence on nonradiative dot density, another CdSe/ZnS sample degraded by exposure to air in a refrigerator for several months was also prepared. The fluorescence peak of this sample was 2.08 eV (597 nm) with an inhomogeneous distribution of 24 meV.

IV. ANALYSIS AND DISCUSSION

We first measured the fresh QD sample. Figure 5(a) shows the spectrally integrated fluorescence intensity for various temperatures. The excitation photon energy is set to $E_{\rm exc} =$ 2.76 eV, which is much higher than the absorption edge, so that all the QDs are assumed to be excited irrespective of their size. The fluorescence lifetime of the QD array is generally shorter than that of the QD dispersion and tends to decrease as the temperature increases. In previous studies, we showed that this lifetime shortening can be attributed to excitons hopping to a quenching site (dark QD) that exhibits fast nonradiative decay.[19,20] To quantify the hopping dynamics, we first extract $\rho(t)$ from the experimental results. Since the fluorescence intensity is proportional to the exciton population, the measured fluorescence intensity at time t after a pulse excitation $I(t)$ is related to the survival probability $\rho(t)$

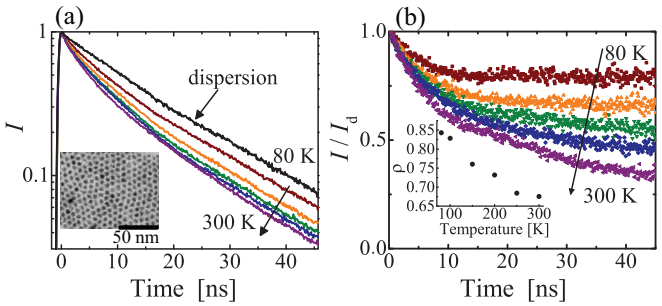

FIG. 5. (Color online) (a) Time-resolved fluorescence intensities $I(t)$ of the QD arrays of fresh QDs at 80, 150, 200, 250, and 300 K. The fluorescence decay curve of the QD dispersion at 80 K is also shown for comparison. The inset shows a TEM image of QDs forming a 2D close-packed network with hexagonal order, where a carbon thin film was used as a sample plate instead of quartz. The average diameter and interdot distance of the QD array were 5.2 and 7.9 nm, respectively. (b) Time courses of the survival probability $\rho(t) = I(t)/I_d(t)$ at 80, 150, 200, 250, and 300 K. The inset shows the fraction of excitons $\tilde{\rho}$ that decay in the bright QDs instead of reaching dark sites.

through

$$I(t) = I_0 \left\langle \exp\left[-\left(\sum_{i=0}^{N_{\rm hops}} k_i \tau_i \right) \right] \right\rangle \rho(t), \tag{12}$$

where i denotes the sequence of the sites visited, τ_i is the time spent at the ith site satisfying the relation $\sum_i^{N_{\rm hops}} \tau_i = t$, $N_{\rm hops}$ is the total number of hops that occur before t, and $k_{\rm i}$ is the exciton decay rate at the ith (bright) site, which is assumed to be much smaller than that at the dark site. In the QD ensemble, the exciton lifetime is considered to vary from QD to QD, even for bright QDs, because of inhomogeneity or fluctuations in the nonradiative relaxation pathways,[50] and therefore the fluorescence decay of the QD ensemble does not usually follow a single exponential function. Since $\langle \exp[-(\sum_{i=0}^{N_{\rm hops}} k_i \tau_i)] \rangle = \langle \exp[-(k_n t)] \rangle_n$, with $\langle \cdots \rangle_n$ being the ensemble average over site n, Eq. (12) can be rewritten as

$$I(t) = I_{\rm d}(t)\rho(t), \tag{13}$$

where $I_d(t) = I_0 \langle \exp[-(k_n t)] \rangle_{\rm n}$ denotes the fluorescence intensity of the QD ensemble in the absence of exciton hopping. Therefore, $\rho(t)$ is obtained by dividing $I(t)$ by $I_d(t)$, which can be measured from the QD ensemble in the dispersed state.

Figure 5(b) shows how $\rho(t) = I(t)/I_{\rm d}(t)$ decreases as the temperature increases. We find that, at 80 K, $\rho(t)$ remains nearly constant after ~10 ns. In contrast, at high temperatures, $\rho(t)$ continues to decrease even after 40 ns. These trends agree with the results of the numerical simulations shown in Fig. 1(b). The inset in Fig. 5(b) shows the fraction of excitons $\tilde{\rho}$ that decay radiatively or nonradiatively in bright QDs instead of reaching dark sites. This fraction is given by

$$\tilde{\rho} = \int_0^\infty I(t)dt \Big/ \int_0^\infty I_{\rm d}(t)dt, \tag{14}$$

from which it is clear that $\tilde{\rho}$ decreases as the temperature increases.

We can estimate γ via Eq. (11) using $S_{\rm inf}$ and $\rho_{\rm inf}$. Figure 6(a) shows time courses of $\rho(t)$ at low temperature

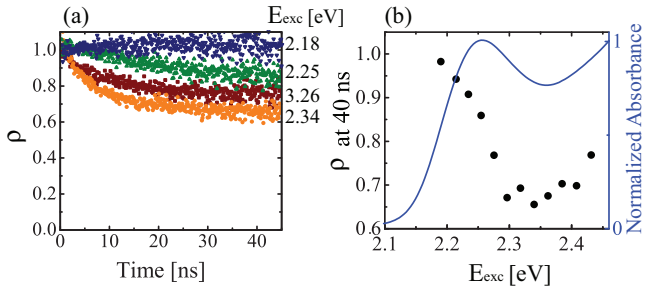

FIG. 6. (Color online) (a) Time courses of the survival probability $\rho(t)$ for various excitation photon energies $E_{\rm exc}$. The temperature is 80 K. (b) Asymptotic values of $\rho(t)$ (at $t = 40$ ns) as a function of $E_{\rm exc}$. The absorption spectrum of the QD dispersion measured at 110 K is also shown as the solid line.

(80 K) for various values of $E_{\rm exc}$. Although the temperature is not zero and $\rho(t)$ is still decreasing slightly at 40 ns, the rate of change is small. Therefore, we approximate $\rho_{\rm inf}$ by $\rho(t)$ at $t = 40$ ns. Figure 6(b) shows the corresponding $\rho_{\rm inf}$ as a function of $E_{\rm exc}$, and the absorption spectrum measured at 110 K is also shown. We find that $\rho_{\rm inf}$ has a minimum when $E_{\rm exc}$ is around 2.34 eV. In this case, high-energy QDs are considered to be selectively excited since $E_{\rm exc}$ is slightly higher than the first absorption peak at 2.25 eV. By setting $\rho_{\rm inf} = 0.65$ and $S_{\rm inf} = 2.75$ on the assumption that the QDs form a 2D array with hexagonal order, γ is estimated to be 0.14.

We note that when $E_{\rm exc}$ is much higher than the absorption edge at 3.26 eV, all the QDs are considered to be excited equally, irrespective of their energy level. In this case, $\rho_{\rm inf}$ is found to be 0.76. From this value and assuming the numerical result $S_{\rm inf} = 1.81$, γ can be estimated as 0.14, which agrees with the value obtained when high-energy QDs are selectively excited. It should also be noted that when $E_{\rm exc}$ is set to the energy of the absorption edge, 2.18 eV, then $\rho(t)$ remains close to unity. In this case, low-energy QDs are selectively excited, and excitons tend to be trapped at the initial site.

We then calculated $\langle S(t)\rangle^*$ by substituting $\rho(t)$ and γ into Eq. (3) [Fig. 7(a)]. Approximate values of the normalized

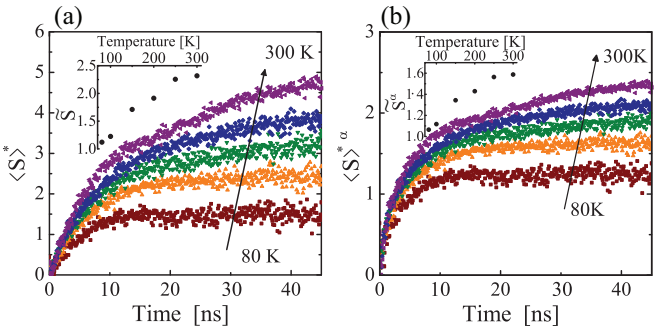

FIG. 7. (Color online) (a) Average number of distinct sites visited, $\langle S(t)\rangle^*$, and (b) approximate values of the average hopping distance normalized by the interdot distance, $\langle S(t)\rangle^{*\alpha}$, for various temperatures ($T = 80$, 150, 200, 250, and 300 K). We set $\gamma = 0.14$ and $\alpha = 0.56$. The inset in panel (a) shows the average number of distinct sites visited before exciton decay at any site $\tilde{S}$, and the inset in panel (b) is the approximate value of the normalized hopping distance before exciton decay $\tilde{S}^{\alpha}$.

average hopping distances $\langle S(t)\rangle^{*\alpha}$ obtained at various temperatures are shown in Fig. 7(b). Here, we set $\gamma = 0.14$ and $\alpha = 0.56$. At 80 K, $\langle S(t)\rangle^*$ and $\langle S(t)\rangle^{*\alpha}$ are almost saturated after 10 ns. In contrast, at 300 K, $\langle S(t)\rangle^*$ and $\langle S(t)\rangle^{*\alpha}$ take values of 4.8 and 2.4, respectively, and continue to increase after 40 ns. These results indicate that an exciton is preferentially trapped in a local low-energy site at low temperature, while at room temperature, hopping repeatedly occurs and leads to a long hopping distance. This is consistent with our previous experimental findings, in which the initial fluorescence rise appears in the low-energy region only at low temperatures and the magnitude of the redshift markedly increases with decreasing temperature.[19] It should be noted that $\langle S(t)\rangle^*$ and $\langle S(t)\rangle^{*\alpha}$ in Fig. 7 correspond to the case when radiative or nonradiative decay at a bright site is not considered; an exciton eventually reaches a dark site at a finite temperature, and the asymptotic values of $\langle S(t)\rangle^*$ and $\langle S(t)\rangle^{*\alpha}$ in the long-time limit are expected to be $1/\gamma = 7.1$ and $1/\gamma^{\alpha} = 2.9$, respectively. However, an exciton can also decay at a bright site before it reaches a dark site. The average number of distinct sites visited before an exciton decays at either a bright or dark site is given by

$$\tilde{S} = \int_0^{\infty} \langle S(t)\rangle^* I_{\rm d}(t)dt \Big/ \int_0^{\infty} I_{\rm d}(t)dt. \qquad (15)$$

From Eqs. (3), (13), and (14), Eq. (15) can be rewritten as $\tilde{S} = (1-\tilde{\rho})/\gamma$. The insets in Figs. 7(a) and 7(b) show $\tilde{S}$ and $\tilde{S}^{\alpha}$ as a function of temperature, where the latter is given by replacing $\langle S(t)\rangle^*$ in Eq. (15) with $\langle S(t)\rangle^{*\alpha}$ and denotes an approximate hopping distance before exciton decay at any site.

We also measured the time-resolved fluorescence intensity of a degraded QD sample that contained a large number of dark QDs. Figure 8 shows that, in the initial stage, there is a fast decay component that originates from the dark QDs. The curves, fit with an exponential and offset $I(t) = a_1\exp(-t/\tau) + a_2$, suggest that the decay time of the fast component is $\tau = 0.22$ ns, which is comparable to that of the off state CdSe/CdZnS QD, 0.25 ns, measured by means of single-molecule spectroscopy.[51] The amplitudes (a_1 and a_2) are related to the relative proportions of dark and bright QDs, and γ is obtained as $\gamma = a_1/(a_1 + a_2) = 0.64$. However, for a fresh sample, this method is considered to be unreliable,

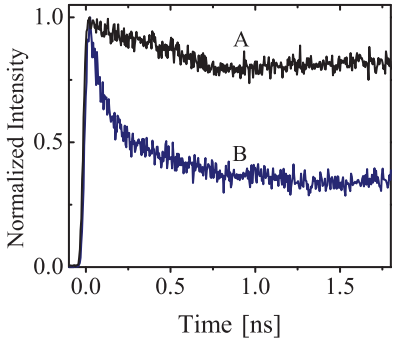

FIG. 8. (Color online) Time-resolved fluorescence intensities of a (A) fresh and (B) degraded sample in the initial stages. The samples are dissolved in toluene, and the measurement was performed under room-temperature conditions. The excitation photon energy was 3.26 eV.

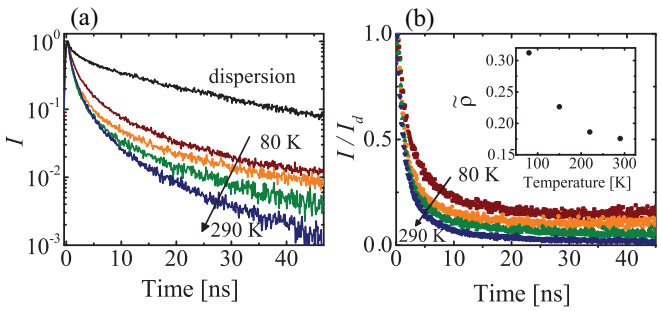

FIG. 9. (Color online) (a) Time-resolved fluorescence intensities $I(t)$ of a QD array of degraded QDs at 80, 150, 220, and 290 K. The fluorescence decay curve of the QD dispersion at room temperature is also shown for comparison. (b) Time courses of the survival probability $\rho(t) = I(t)/I_d(t)$ at 80, 150, 220, and 290 K. The inset shows the fraction of excitons, $\tilde{\rho}$, that decay at bright QDs instead of reaching dark sites.

since the fluorescence intensity is nearly flat in the initial stage. In the case of small γ, we can estimate γ by measuring the time-resolved fluorescence intensities at low temperature, as described above. We confirmed that the decay profiles in the initial stage are nearly independent of temperature, thus indicating that γ is independent of temperature.

Figures 9(a) and 9(b) show the time-resolved fluorescence intensities of a QD array that consists of degraded QDs and the calculated survival probability for various temperatures, respectively. The fluorescence intensities and survival probability decrease with increasing temperature, and it should be noted that the survival probability significantly decreases after about 10 ns. This trends agrees with the results of the numerical simulation shown in Fig. 1(c) and suggests that a large number of excitons reach a dark QD followed by quenching.

Figure 10(a) shows $\langle S(t)\rangle^*$ and $\langle S(t)\rangle^{*\alpha}$ as calculated using the $\rho(t)$ data in Fig. 9(b). Here, we set $\gamma = 0.64$ and $\alpha = 0.56$. Even though these quantities increase with increasing temperature, they are more-or-less saturated after about 10 ns. This indicates that a large number of the excitons are quenched at a dark QD in the vicinity of the initial site.

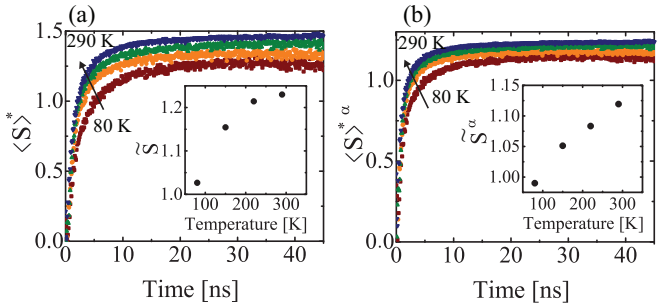

FIG. 10. (Color online) (a) Average number of distinct sites visited, $\langle S(t)\rangle^*$, and (b) approximate values of the average hopping distance normalized by the interdot distance, $\langle S(t)\rangle^{*\alpha}$, for various temperatures ($T = 80$, 150, 220, and 290 K). The sample is a QD array consisting of degraded QDs, and we set $\gamma = 0.64$ and $\alpha = 0.56$. The inset in panel (a) shows the average number of distinct sites visited before the exciton decays at any site $\tilde{S}$, and the inset in panel (b) is the approximate value of the normalized hopping distance before exciton decay $\tilde{S}^{\alpha}$.

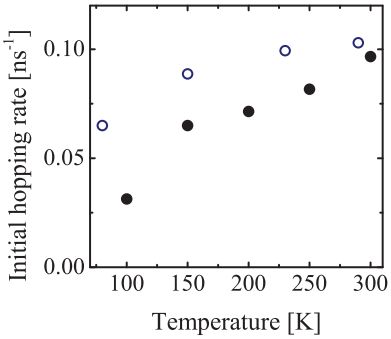

FIG. 11. (Color online) Average hopping rates in the initial stage as a function of temperature. Filled and open circles are the rates of the QD array consisting of fresh and degraded QDs, respectively.

To further quantify the exciton dynamics, we estimated the average hopping rate $w_{\rm int}$ in the initial stage, which is related to the rate of change of $S(t)$ and N by

$$w_{\rm int} = \frac{1}{N}\frac{dS(t)}{dt}\bigg|_{t=0}. \tag{16}$$

Figure 11 shows $w_{\rm int}$ obtained using the linear fit of $S(t)$ from 0 to 1.5 ns in Figs. 7(a) and 10(a). We set $N = 6$, assuming that the QDs form a 2D hexagonal lattice. We can see clearly that $w_{\rm int}$ increases with increasing in temperature. The $w_{\rm int}$ of the QD array consisting of degraded QDs is larger than that of the fresh QD array. This is presumably attributed to the difference in the width of the inhomogeneous distribution (33 meV for the fresh sample and 24 meV for the degraded sample employed in this study), since the average hopping rate is considered to increase as the inhomogeneous width decreases.

A few issues should be discussed to further understand the experimental results. Here and in previous studies, we considered a dark QD in view of the fact that an individual QD usually exhibits intermittent switching between the dark (off) and bright (on) states due to defects or excess charges on the QD surface.[50–54] The fluorescence intensity of a blinking QD is generally correlated with its decay time;[50,51,54] for example, Rosen *et al.*[51] have observed that the fluorescence decay time of an off-state CdSe/CdZnS QD is 250 ps,[51] which is much faster than that of an on-state QD (around tens of nanoseconds) and the exciton hopping rate (around several nanoseconds, when exciton hopping occurs from a high- to low-energy site[19]). In this study, we estimated γ to be 0.14 for the fresh sample by means of site-selective excitation at low temperature, and this value is consistent with our previous studies in which the numerical simulation using the master equations agreed with the experimental results when γ was around 0.2.[19,20] In contrast, we estimated γ to be 0.64 for the degraded sample from the fast decay component of the time-resolved fluorescence intensity. To gain further insight into the origin and mechanism of a dark QD, it is worthwhile examining the relationship between γ and the ratio of the time interval between on and off states. Measurements of individual QDs will be one promising approach for this purpose.

In analyzing the experimental data, some parameters ($S_{\rm inf}$ and α) were obtained from the numerical simulation with the assumption that the QD array forms a 2D lattice with hexagonal order; the configuration of a QD array can be

identified by means of electron microscopy or x-ray analysis. To apply the present method to QD arrays with different lattice configurations,[55] it is necessary to obtain parameter values specific to each configuration, but these parameter values do not seem to be sensitive to the lattice configuration in dimensions higher than or equal to two. In this regard, the TEM image in the inset of Fig. 5(a) may not be representative of the sample that is measured optically, since a carbon thin film was used as the sample plate for the TEM observation as opposed to quartz. However, we believe that this does not make much difference to the analytical results presented in this study as long as the dimensions of the QD array are higher than or equal to two. We verified this by preparing QDs in an ethyl acetate solution in which the QDs aggregate and yield a turbid solution. In this case, the QDs are considered to form a 3D structure, which is different to that formed on the quartz plate. We also prepared a QD film on quartz by means of dip coating in addition to the drop-casting technique. We confirmed that fluorescence decay profile of these samples does not show a large difference in comparison with the results related to the drop-cast structure on quartz. For example, the fluorescence lifetimes of the QD aggregate in ethyl acetate, dip-coated QD film, and drop-cast QD film are 10.9, 11.7, and 11.4 ns, respectively.

Finally, we discuss the potential applicability of this analytical method to other systems. For example, for doped, disordered organic semiconductors such an alkoxy-substituted poly phenylenevinylene (PhPPV) doped with trinitrofluorene (TNF), the doped molecule serves as a electron acceptor at which an exciton dissociates.[56] Since the doped molecules are located next to the host molecules, the probability of an exciton encountering the electron acceptor is determined by the number of host sites visited. In a similar manner to the present study, the survival probability is given by Eq. (13) by substituting in the time-resolved fluorescence intensities detected from the sample with and without the doping molecules. Furthermore, Eq. (3) is considered to be valid for such a system provided that the doped molecules are randomly distributed and the exciton dissociation rate is much larger than the hopping rate. However, it would be necessary to reexamine the relationship between the average number of distinct sites visited and the hopping distance, since the distance between neighboring sites is not constant but randomly distributed. Thus, further study is needed to extend our analytical method to provide a better understanding of relevant systems in addition to nanocrystals.

V. CONCLUSION

We have described an analytical method that quantifies exciton hopping in disordered media with quenching sites. On the basis of Monte Carlo simulations, we showed that the relationship among several statistical quantities characterizes the dynamics (survival probability, average number of distinct sites visited, and average hopping distance). This method was subsequently used to describe the exciton hopping dynamics in a QD array in a qualitative way. The survival probability was extracted from the time-resolved fluorescence intensities. To calculate the average number of sites visited from the survival probability, it is necessary to determine the proportion of quenching sites (dark QD) that exhibit fast decay. We showed that, when the proportion of quenching sites is small, it can be quantified by means of site-selective excitation at low temperature. The average number of distinct sites visited was then obtained through Eq. (3), while an approximate value of the hopping distance was given by Eqs. (7) or (9), depending on the dimensions and lattice configuration. We also estimated the average hopping rate in the initial stage. The temperature dependence of these statistical quantities showed clearly that at low temperature the exciton tends to be trapped at a local low-energy site, while at room temperature, exciton hopping occurs repeatedly leading to a large hopping distance.

ACKNOWLEDGMENTS

The author thanks Shuichi Kinoshita of the Graduate School of Frontier Biosciences, Osaka University, for permitting the use of the experimental system and providing helpful suggestions. This work was partially supported by a Grant-in-Aid for Scientific Research (No. 24740261) received from the Japan Society for the Promotion of Science.

APPENDIX A

We consider the probability distribution $\theta_s(l)$ of a random walker that visits the sth distinct site that is located at a distance l relative to the initial site. Here, l is normalized by the interdot distance d. For a 1D system, $\theta_s(l)$ satisfies the following recurrence relation:

$$\theta_s(l) = \omega_{s-1}^{l,l-1}\theta_{s-1}(l-1) + \omega_{s-1}^{l,s-l}\theta_{s-1}(s-l), \tag{A1}$$

where $\omega_{s-1}^{l,l-1(s-l)}$ is the transition probability that a random walker that has visited the $(s-1)$st distinct site at $l-1$ $(s-l)$ will next visit the sth distinct site at l. In other words, Eq. (A1) means that random walkers at the $(s-1)$st step at $l-1$ (the neighboring site) and $s-l$ (the opposite end site) contribute to the next sth step at l. When the hopping probability is constant for all pairs of neighboring sites, the transition probabilities are written as

$$\begin{aligned} \omega_{s-1}^{l,l-1} &= s/(s+1), \\ \omega_{s-1}^{l,s-l} &= 1/(s+1), \end{aligned} \tag{A2}$$

and the solution for Eq. (A1) is given by

$$\theta_s(l) = l \Big/ \sum_{n=1}^{s} n. \tag{A3}$$

The hopping distance of random walkers averaged over l while holding s constant is then calculated to be

$$\begin{aligned} \langle L\rangle_s &= d\sum_{l=1}^{s} l\theta_s(l) \\ &= d[(2/3)s + 1/3]. \end{aligned} \tag{A4}$$

APPENDIX B

The number of distinct sites visited in the long-time limit at zero temperature is related to the energy levels among the sites. The probability distribution ϕ_s of a random walker that

has visited the sth distinct site in the long-time limit is written in the 1D system as

$$\phi_s = \tilde{\phi}_s \left[2 \int_{\epsilon}^{\infty} P(\epsilon') d\epsilon' + \int_{-\infty}^{\epsilon} P(\epsilon') d\epsilon' \right], \quad \text{(B1)}$$

with

$$\tilde{\phi}_s = \int_{-\infty}^{\epsilon} P(\epsilon_1) d\epsilon_1 \int_{-\infty}^{\epsilon_1} P(\epsilon_2) d\epsilon_2 \times \cdots \int_{-\infty}^{\epsilon_{s-1}} P(\epsilon_s) d\epsilon_s \int_{\epsilon_s}^{\infty} P(\epsilon_{s+1}) d\epsilon_{s+1}, \quad \text{(B2)}$$

where ϵ is the energy level of the initial site, and $P(\zeta)$ is the inhomogeneous distribution of the site energy ζ, for which we have assumed a Gaussian distribution with a width of σ and an average of zero:

$$P(\zeta) = \frac{1}{\sqrt{2\pi}\sigma} \exp\left[-\frac{\zeta^2}{2\sigma^2} \right]. \quad \text{(B3)}$$

The long-time limit of $\langle S(t) \rangle$ at zero temperate S_{inf} is written as

$$S_{\text{inf}} = \sum_{s=1}^{\infty} s \phi_s. \quad \text{(B4)}$$

Equation (10) is obtained by substituting Eqs. (B1), (B2), and (B3) into Eq. (B4).

*miyazaki@ils.uec.ac.jp

[1] I. Gur, N. A. Fromer, M. L. Geier, and A. P. Alivisatos, Science **310**, 462 (2005).
[2] S. A. McDonald, G. Konstantatos, S. Zhang, P. W. Cyr, E. J. D. Klem, L. Levina, and E. H. Sargent, Nat. Mater. **4**, 138 (2005).
[3] J. Y. Kim, K. Lee, N. E. Coates, D. Moses, T. Nguyen, M. Dante, and A. J. Heeger, Science **13**, 222 (2007).
[4] V. L. Colvin, M. C. Schlamp, and A. P. Alivisatos, Nature (London) **370**, 354 (1994).
[5] S. Coe, W. K. Woo, M. Bawendi, and V. Bulović, Nature (London) **420**, 800 (2002).
[6] M. Achermann, M. A. Petruska, D. D. Koleske, M. H. Crawford, and V. I. Klimov, Nano Lett. **6**, 1396 (2006).
[7] T. Kim, K. Cho, E. K. Lee., S. J. Lee, J. Chae, J. W. Kim, D. H. Kim, J. Kwon, G. Amaratung, S. Y. Lee, B. Y. Choi, Y. Kuk, J. M. Kim, and K. Kim, Nat. Photonics **5**, 176 (2011).
[8] D. S. Ginger and N. C. Greenham, J. Appl. Phys. **87**, 1361 (2000).
[9] G. Konstantatos, I. Howard, A. Fischer, S. Hoogland, J. Clifford, E. Klem, L. Levina, and E. H. Sargent, Nature (London) **442**, 180 (2006).
[10] D. C. Oertel, M. G. Bawendi, A. C. Arango, and V. Bulovic, Appl. Phys. Lett. **87**, 213505 (2005).
[11] C. R. Kagan, C. B. Murray, M. Nirmal, and M. G. Bawendi, Phys. Rev. Lett **76**, 1517 (1996).
[12] O. I. Mićić, K. M. Jones, A. Cahill, and A. J. Nozik, J. Phys. Chem. B **102**, 9791 (1998).
[13] S. A. Crooker, J. A. Hollingsworth, S. Tretiak, and V. I. Klimov, Phys. Rev. Lett **89**, 186802 (2002).
[14] T. Franzl, A. Shavel, A. L. Rogach, N. Gaponik, T. A. Klar, and A. Eychmuller, Small **1**, 392 (2005).
[15] D. G. Kim, S. Okahara, M. Nakayama, and Y. G. Shim, Phys. Rev. B **78**, 153301 (2008).
[16] M. Lunz, A. L. Bradley, V. A. Gerard, S. J. Byrne, Y. K. Gunko, V. Lesnyak, and N. Gaponik, Phys. Rev. B **83**, 115423 (2011).
[17] M. Lunz, A. L. Bradley, W. Y. Chen, V. A. Gerard, S. J. Byrne, Y. K. Gunko, V. Lesnyak, and N. Gaponik, Phys. Rev. B **81**, 205316 (2010).
[18] C. Higgins, M. Lunz, A. L. Bradley, V. A. Gerard, S. Byrne, Y. K. Gun'ko, V. Lenyak, and N. Gaponik, Opt. Exp. **18**, 24486 (2010).
[19] J. Miyazaki and S. Kinoshita, J. Phys. Soc. Jpn. **81**, 074708 (2012).
[20] J. Miyazaki and S. Kinoshita, Phys. Rev. B **86**, 035303 (2012).
[21] D. F. O'Briena, M. A. Baldo, M. E. Thompson, and S. R. Forrest, Appl. Phys. Lett. **74**, 442 (1999).
[22] V. I. Arkhipov, E. V. Emelianova, and H. Bässler, Phys. Rev. B **70**, 205205 (2004).
[23] V. M. Burlakov, K. Kawata, H. E. Assender, G. A. D. Briggs, A. Ruseckas, and I. D. W. Samuel, Phys. Rev. B **72**, 075206 (2005).
[24] S. Athanasopoulos, E. V. Emelianova, A. B. Walker, and D. Beljonne, Phys. Rev. B **80**, 195209 (2009).
[25] C. Bardeen, Science **331**, 544 (2011).
[26] R. Berera, C. Herrero, I. H. M. van Stokkum, M. Vengris, G. Kodis, R. E. Palacios, H. van Amerongen, R. van Grondelle, D. Gust, T. A. Moore, A. L. Moore, and J. T. M. Kennis, Proc. Natl. Acad. Sci. U. S. A. **103**, 5343 (2006).
[27] R. Berera, I. H. van Stokkum, S. d'Haene, J. T. Kennis, R. van Grondelle, and J. P. Dekker, Biophys. J. **96**, 2261 (2009).
[28] N. E. Holt, D. Zigmantas, L. Valkunas, X. P. Li, K. K. Niyogi, and G. R. Fleming, Science **21**, 433 (2005).
[29] Y. Roichman and N. Tessler, Appl. Phys. Lett. **80**, 1948 (2002).
[30] J. van de Lagemaat, Phys. Rev. B **72**, 235319 (2005).
[31] K. Harada, A. G. Werner, M. Pfeiffer, C. J. Bloom, C. M. Elliott, and K. Leo, Phys. Rev. Lett. **94**, 036601 (2005).
[32] A. V. Nenashev, F. Jansson, S. D. Baranovskii, R. Österbacka, A. V. Dvurechenskii, and F. Gebhard, Phys. Rev. B **81**, 115204 (2010).
[33] G. A. H. Wetzelaer, L. J. A. Koster, and P. W. M. Blom, Phys. Rev. Lett. **107**, 066605 (2011).
[34] B. Movaghar, M. Grünewald, B. Ries, H. Bässler, and D. Würtz, Phys. Rev. B **33**, 5545 (1986).
[35] T. M. Nieuwenhuizen, Phys. Rev. Lett. **62**, 357 (1989).
[36] C. Sire, Phys. Rev. E **60**, 1464 (1999).
[37] C. Texier and C. Hagendorf, Europhys. Lett. **86**, 37011 (2009).
[38] P. L. Doussal, J. Stat. Mech. (2009) P07032.
[39] H. B. Rosenstock, J. Math. Phys. **11**, 487 (1970).
[40] M. D. Donsker and S. R. S. Varadhan, Commun. Pure Appl. Math. **28**, 525 (1975).
[41] A. Blumen and G. Zumofen, J. Chem. Phys. **77**, 5127 (1982).
[42] G. Zumofen and A. Blumen, J. Chem. Phys. **76**, 3713 (1982).
[43] J. Haus and K. W. Kehr, Phys. Rep. **150**, 263 (1987).
[44] J. Schotland, J. Chem. Phys. **88**, 907 (1988).
[45] H. Larralde, P. Trunfio, S. Havlin, H. E. Stanley, and G. H. Weiss, Phys. Rev. A **45**, 7128 (1992).

[46]L. K. Gallos, P. Argyrakis, and K. W. Kehr, Phys. Rev. E **63**, 021104 (2001).
[47]G. T. Barkema, P. Biswas, and H. van Beijeren, Phys. Rev. Lett. **87**, 170601 (2001).
[48]C. Madigan and V. Bulović, Phys. Rev. Lett. **96**, 046404 (2006).
[49]K. Feron, W. J. Belcher, C. J. Fell, and P. C. Dastoor, Int. J. Mol. Sci. **13**, 17019 (2012).
[50]B. R. Fisher, H.-J. Eisler, N. E. Stott, and M. G. Bawendi, J. Phys. Chem. B **108**, 143 (2004).
[51]S. Rosen, O. Schwartz, and D. Oron, Phys. Rev. Lett. **104**, 157404 (2010).
[52]M. Nirmal, B. O. Dabbousi, M. G. Bawendi, J. J. Macklin, J. K. Trautman, T. D. Harris, and L. E. Brus, Nature (London) **383**, 802 (1996).
[53]A. L. Efros and M. Rosen, Phys. Rev. Lett. **78**, 1110 (1997).
[54]C. Galland, Y. Ghosh, A. Steinbrück, M. Sykora, J. A. Hollingsworth, V. I. Klimov, and H. Htoon, Nature (London) **479**, 203 (2011).
[55]C. B. Murray, C. R. Kagan, and M. G. Bawendi, Science **24**, 1335 (1995).
[56]C. Im, J. M. Lupton, P. Shouwink, S. Heun, and H. Becker, J. Chem. Phys. **117**, 1395 (2002).